DNA vaccines targeting amyloid-β oligomer ameliorate cognitive deficits of aged APP/PS1/tau triple-transgenic mouse models of Alzheimer's disease

https://doi.org/10.4103/1673-5374.337054

Date of submission: July 5, 2021

Date of decision: October 18, 2021

Date of acceptance: December 15, 2021

Date of web publication: February 28, 2022

Sha Sha[1], Xiao-Na Xing[2], Tao Wang[3], Ying Li[1], Rong-Wei Zhang[1], Xue-Li Shen[1], Yun-Peng Cao[4], Le Qu[5, *]

From the Contents

Graphical Abstract *DNA vaccine is a strong candidate in the treatment and prevention of early Alzheimer's disease*

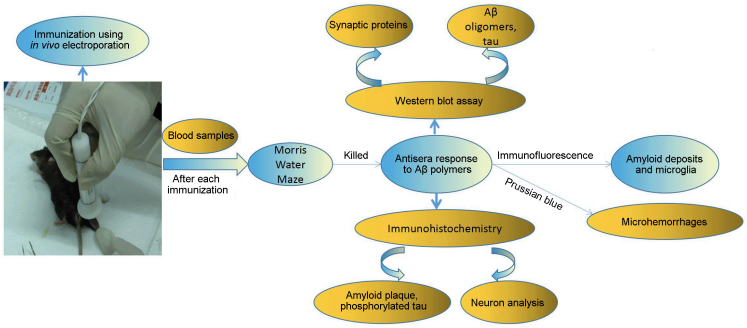

Abstract

The amyloid-β (Aβ) oligomer, rather than the Aβ monomer, is considered to be the primary initiator of Alzheimer's disease. It was hypothesized that p(Aβ3–10)10-MT, the recombinant Aβ3–10 gene vaccine of the Aβ oligomer has the potential to treat Alzheimer's disease. In this study, we intramuscularly injected the p(Aβ3–10)10-MT vaccine into the left hindlimb of APP/PS1/tau triple-transgenic mice, which are a model for Alzheimer's disease. Our results showed that the p(Aβ3–10)10-MT vaccine effectively reduced Aβ oligomer levels and plaque deposition in the cerebral cortex and hippocampus, decreased the levels tau protein variants, reduced synaptic loss, protected synaptic function, reduced neuron loss, and ameliorated memory impairment without causing any cerebral hemorrhaging. Therefore, this novel DNA vaccine, which is safe and highly effective in mouse models of Alzheimer's disease, holds a lot of promise for the treatment of Alzheimer's disease in humans.

Key Words: Aβ oligomers; cognitive dysfunction; DNA vaccine; immunotherapy; neuron loss; plaque deposits; synaptic function; tau hyperphosphorylation

Introduction

The amyloid-β (Aβ) oligomers are viewed as the causative agent of Alzheimer's disease (AD) and can induce a series of pathophysiological changes such as tau hyperphosphorylation, inflammation, oxidative stress, synaptic dysfunction, and neurodegeneration (Sevigny et al., 2016; Yepes, 2021; Zhang et al., 2021). Both active and passive immunotherapies can effectively eliminate amyloid deposits and the pathophysiological changes induced by Aβ in human and animal models (Godyń et al., 2016; Martinez and Peplow, 2019). Monoclonal antibodies such as solanezumab, gantenerumab, crenezumab, and aducanumab specifically directed against the most neurotoxic Aβ forms are undergoing large-scale trials to confirm initially encouraging results in the mild cognitive impairment stage and in patients at high risk of developing AD (Panza et al., 2019). However, in a previous study, there was no evidence of improved survival or time to severe dementia in the AN1792 clinical trial group versus the placebo group (Holmes et al., 2008).

Currently, the lack of a specific treatment that targets the most toxic oligomers may be the major setback in immunotherapy because targeting normal soluble Aβ can interfere with its crucial physiological functions, including neuroprotection, modulation of synaptic elasticity, memory consolidation, and maintenance of innate immunity (Palmeri et al., 2017). Anti-Aβ oligomer therapies have also reduced tau pathology in animal disease models (Nisbet et al., 2015). In a recent study, a strong interaction between soluble Aβ and tau has been shown in the AD pathocascade prior to their deposition as plaques and neurofibrillary tangles, respectively, with tau acting downstream of Aβ. The Aβ oligomer binds to the plasma membrane, opens calcium channels and downregulates the activation of phosphokinases implicated in tau phosphorylation. Aβ can mediate the activation of extrasynaptic N-methyl D aspartate receptors, which in turn activate kinases such as AMPK. Activated kinases can phosphorylate dendritic tau, which then results in the migration of tau and Fyn into the dendritic spine (Nisbet et al., 2015). As the disease progresses, Aβ is thought to activate a striatal-enriched protein tyrosine phosphatase, eventually leading to synaptic loss and dendrite collapse. Furthermore, reducing soluble Aβ without disturbing tau phosphorylation cannot improve cognitive impairment, therefore, saving cognitive impairment in transgenic (Tg) mice requires the reduction of both soluble Aβ and tau levels (Oddo et al., 2006; Mairet-Coello et al., 2013).

Synaptic-associated proteins play an important role in modulating memory conduction. Dynamin 1 plays an important role in the release of synaptic vesicles, and postsynaptic density protein 95 (PSD-95) regulates the maturation and elasticity of synapses. Both proteins can be degraded by calpain activation, which is induced by Aβ accumulation (Fà et al., 2014). Immunotherapy, which can selectively decrease the number of soluble Aβ oligomers, as well as reduce the loss of synaptic-related proteins, will help further protect spatial memory and synaptic function (Loureiro et al., 2020). Soluble Aβ oligomers begin to damage synaptic function and affect cognition

[1]Department of Geriatrics, the First Affiliated Hospital of China Medical University, Shenyang, Liaoning Province, China; [2]Department of Neurology, Shenzhen Luohu People's Hospital, The Third Affiliated Hospital of Shenzhen University, Shenzhen, Guangdong Province, China; [3]College of Life and Health Sciences, Northeastern University, Shenyang, Liaoning Province, China; [4]Department of Neurology, the First Affiliated Hospital of China Medical University, Shenyang, Liaoning Province, China; [5]Department of Dermatology, the First Affiliated Hospital of China Medical University, Shenyang, Liaoning Province, China

*Correspondence to: Le Qu, PhD, cmuqule@163.com.

https://orcid.org/0000-0002-6923-5364 (Le Qu)

Funding: *This study was supported by the National Nature Science Foundation of China, No. 81870819 (to YPC); and the Natural Science Foundation of Liaoning Province of China, No. 2019-MS-200 (to XNX).*

How to cite this article: *Sha S, Xing XN, Wang T, Li Y, Zhang RW, Shen XL, Cao YP, Qu L (2022) DNA vaccines targeting amyloid-β oligomer ameliorate cognitive deficits of aged APP/PS1/tau triple-transgenic mouse models of Alzheimer's disease. Neural Regen Res 17(10):2305-2310.*

from the onset of AD before plaque deposition, thus, early intervention in the disease is necessary to obtain the most significant benefits. The triple-Tg mouse (3×Tg-AD, harboring *APPSwe* and *tau*^{P301L} transgenes in a mutant *PS1*^{M146V} knock-in background) represents a unique model that develops both Aβ plaques and neurofibrillary tangles before exhibiting deficits in synaptic plasticity that closely mimic their development in the human AD brain (Yu et al., 2018).

In the present study, the immune characterization of 3×Tg-AD mice immunized with a recombinant $Aβ_{3–10}$ gene vaccine and its efficacy on AD-related pathology were investigated. Finally, the relationship between tau and Aβ and its effect on synaptic function were discussed, providing a strong basis for further investigation on the effects of Aβ gene vaccines.

Materials and Methods

Animals

Breeding pairs of homozygous 3×Tg-AD mice (*n* = 20, 4 months of age, 10 males and 10 females, RRID: 004807) were purchased from Jackson Laboratory (Farmington, ME, USA). Ten C57/B6 mice (five female and five male) of the same age were purchased from Beijing Vital River Laboratory Animal Technology Co., Ltd., China (license No. SYXK (Liao) 2018-0008) as wild-type (WT) mice. The mice were raised in a sterile environment at the Laboratory Animal Centre of China Medical University under 12-hour light/dark, 20–22°C and 40–70% humidity conditions. In addition, experiments were performed according to the guidelines of the Animal Care and Use Committee of the China Medical University. The animal protocol was approved by the Animal Care and Ethics Committee of the First Affiliated of China Medical University (approval No. 2018-220-2) on October 17, 2018. All experiments were designed and reported according to the Animal Research: Reporting of *In Vivo* Experiments (ARRIVE) guidelines (Percie du Sert et al., 2020).

$Aβ_{3–10}$ gene vaccine synthesis and preparation

The gene identified was based on the complementary DNA sequence of gene $Aβ_{3–10}$ in GenBank Fragment synthesis: 5′-TT-EcoRI-Cozak-ATG (initial Bcodon), ($Aβ_{3–10}$)10-TAG (stop codon)-NotI-XhoI-GG-3′, and 10× $Aβ_{3–10}$ were cloned into the pcDNA3.1 mammalian expression vector at the EcoRI and XhoI restriction sites. The recombinant plasmid was confirmed based on NotI/EcoRI digestion and gel electrophoresis. The correct plasmid sequence was confirmed based on nucleotide sequence analysis (Shanghai GeneCore Biotechnology, Shanghai, China). The recombinant plasmid was amplified in DH5 receptive cells of *Escherichia coli* and purified using the E.z.n.^{TM} Fastfilter plasmid-free Maxi kit (OMEGA, Dallas, TX, USA).

Mouse immunization using *in vivo* electroporation

Twenty 3×Tg-AD mice were randomly divided into two groups and immunized with p(Aβ3–10)10-MT vaccine (100 μg, Shanghai Yuchun Biological Technology Company, Shanghai, China) (*n* = 10) or injected with phosphate buffered saline (PBS; 100 μL) (*n* = 10). The PBS-injected mice were used as the negative control group and C57/B6 mice (*n* = 10) were used as the positive control group. The 3×Tg-AD mice (4 months of age) were intramuscularly injected in the left hindlimb with p(Aβ3–10)10-MT vaccine, and each mouse was immunized a total of 10 times with each immunization occurring once every 3 weeks (**Figure 1**). After anesthetization, a pair of 26 gauge electrode needles was inserted 5 mm into the muscle, covering the DNA injection site. Electrical pulses were transmitted using an electric pulse generator (ECM830, BTX, San Diego, CA, USA) with an output of 6.75 V pulses at a rate of 1 pulse per 200 ms (Schommer et al., 2019). Orbital venous blood samples were taken for biochemical examination before the first immunization and 10 days after each immunization. The total number was 10 immunizations, and 1 month after the last immunization, the mice were sacrificed for further experiments. Anesthesia was performed by peritoneal injection of 1% pentobarbital sodium (50 mg/kg, MilliporeSigma, Billerica, MA, USA). The mice were killed, and the brains were quickly removed. Half of each brain was fixed with 4% paraformaldehyde for immunohistochemical staining, and the other half was preserved at –70°C for biochemical index detection.

Immunoreactivity of antisera and response to Aβ polymers

Humoral immune response was detected using enzyme-linked immunosorbent assay (ELISA) (Zhang et al., 2018). In brief, 96-microwell plates were coated with glutathione S-transferase (GST)-Aβ proteins (Wuhan Boster Biological Technology, Wuhan, China) to detect the Aβ peptide in serum samples diluted with PBS at 1:1000. Microtiter wells were treated with blocking buffer (5.0% goat serum, 1% bovine serum albumin, and 0.05% Tween-20 in PBS) and left at room temperature for 2 hours. A standard curve was produced by continuous dilutions of the standard 6E10 antibody (monoclonal anti-Aβ antibody, Cat# SIG-39320, RRID: AB201061, Covance, Princeton, NJ, USA). For western blot analysis, oligomeric Aβ was prepared as described by Dahlgren et al. (2002). The peptide was dissolved in 1 mM hexafluoroisopropanol (MilliporeSigma), which was then removed under vacuum in a vacuum concentrator (Speed Vac, Savant, Holbrook, NY, USA). The remaining peptide was stored in 5 mM dimethyl sulfoxide (MilliporeSigma). Serum-free Ham's F-12 medium (Mediatech, Herndon, VA, USA) with phenol red (100 mL) was added and samples maintained at 4°C for 24 hours. The sample dilution buffer (Boster Biological Technology, Wuhan, China) and 16.5% Tris-tricine sodium dodecyl sulfate polyacrylamide gel electrophoresis separation for NuPage sample. Western blotting was performed using induced anti-sera (6E10, 1 mg/mL, –20°C) and an enhanced chemiluminescence system (Amersham, Arlington Heights, IL, USA) as previously described (Fukuchi et al., 1998).

Morris water maze

The Morris water maze test was used as an assay for cognitive function. It was performed in a circular tank (150 cm in diameter with a 40 cm-high white-stained wall) placed in the center of a quiet room maintained at 22°C as previously described (Wang et al., 2010). The circular tank (Wuhan Yihong Technology Co., Ltd., Wuhan, China) was equipped with a digital pick-up camera to monitor animal behavior and a computer program (XR-XM101, Xinruan Information Technology, Shanghai, China) for data analysis. The Morris water maze test was performed 2 weeks after the last immunization. The mice were trained for 2 days using a visible platform, followed by 2 days using a hidden platform, and then 1 day later a probe test was performed. Each mouse was lowered into the water from each quadrant and was given 60 seconds to reach the platform. In the afternoon of day 5, the platform was removed from the tank and each mouse was allowed a single 60-second probe trial. Finally, data for the escape latency, the times crossing the target platform, and number of crosses over the platform location (Annulus crossing index) in the probe trial were analyzed.

ELISA and immunohistochemistry

The brain of each mouse was homogenized in 10 volumes of guanidine-Tris buffer and mixed for 3 to 4 hours at room temperature. The homogenates were further diluted 1:10 with ice-cold casein buffer before centrifugation (16,000 × *g* for 20 minutes at 4°C). Final dilutions were made in 0.5 M guanidine and 0.1% bovine serum albumin and assessed for Aβ using commercially available ELISA kits (Invitrogen, Camarillo, CA, USA). The absorbance of the plates was read at 450 nm with a spectrophotometer. The right hemisphere was paraffin-embedded to analyze the amyloid plaque burden, and the percentage of the plaque area compared with the total area observed was calculated in two representative images of the cortex and two of the hippocampi (Rajamohamedsait and Sigurdsson, 2012). Aβ plaques were detected using the monoclonal anti-Aβ antibody 6E10. The HT7 antibody that recognizes epitopes 159–163 (Thermo Fisher Scientific, Waltham, MA, USA) was used to detect total tau, and AT8 and AT180 were used to recognize phosphorylated tau levels. AT8 recognizes phosphorylation at the Ser202/Thr205 phosphorylation site and AT180 recognizes phosphorylation at the Thr231 site (Wang et al., 2020). Both cortex and hippocampus were probed for Aβ plaques and tau protein. To better identify neurodegenerative sensitive neurons, the neuron-specific nuclear antigen NeuN antibody (1:3000, mouse monoclonal, Cat# 26975-1-AP, RRID: AB177487, Chemicon, Temecula, CA, USA) was used as marker. Then, the NeuN-probed samples were incubated with horseradish peroxidase-conjugated IgG (1:5000, goat, RRID: AB270144, Cat# SA00001-2, GBI, Bothell, WA, USA). The samples were incubated with primary antibody at room temperature for 1.5 hours. To be representative and accurate, images of the hippocampal CA3 area were analyzed using ImageJ software (1.8.0v) (Schneider et al., 2012) to obtain protein loads (percentage of stained area). The staining was performed on 30 cortical gray matter fields at 20 × magnification from each brain region to determine the number of NeuN-positive neurons in each field. The number of HT7-, AT8-, and AT180-positive neurons was quantified, and the number of pixels (A.U.) represented total tau (HT7) or hyperphosphorylated tau (AT8 and AT180).

Prussian blue staining

To stain microhemorrhages, coronal sections from the left hemispheres of p(Aβ3–10)10-MT and control mice were mounted on gelatin-coated slides and stained with Prussian blue working fluid as previously described (Asuni et al., 2006). Briefly, samples were incubated with equal amounts of distilled H_2O, potassium ferrocyanide, and 20% hydrochloric acid for 30 minutes. The subsequent sections were washed with water, redyed with Nuclear Fast Red solution (N3020, Haoran Biological Technology, Shanghai, China) for 10 minutes, rewashed with water, dehydrated, and covered with a glass slide using Depex mounting media (BDH Laboratory Supplies, Lutterworth, UK).

Immunofluorescence

Activated microglia often show retractions of protuberances, a relative enlargement of their cell bodies, and even macrophage-like appearances. For double immunofluorescence staining to detect any relationship between microglia and Aβ, the frozen sections were placed in fetal bovine serum (1:20) and incubated at room temperature for 1 hour. Sections were incubated overnight at room temperature with the monoclonal anti-Aβ antibody 6E10 (1:1000) and rabbit anti-ionized calcium binding adapter molecule 1 (Iba-1; a microgliosis maker; 1:1000, rabbit, Cat# 66827-1-Ig, RRID: AB178846, Wako, Osaka, Japan). The sections were incubated for 2 hours at room temperature in a mixture of fluorescein isothiocyanate-conjugated goat anti-mouse IgG (1:300, Cat# 15070, RRID: AB150117, Jackson ImmunoResearch Laboratories Inc., West Grove, PA, USA) and Texas red-conjugated goat anti-rabbit IgG (1:5000, Cat# 15071, RRID: AB205718, Abcam, Cambridge, UK) after rinsing with PBS with fluorescein isothiocyanate (Shanghai Guchen Biotechnology Co., Ltd., Shanghai, China) for 2 hours. The sections were then rinsed and covered with PBS/glycerol buffer. The sections were mounted with an anti-fading mounting medium and examined using a confocal laser scanning microscope (SP2; Leica, Wetzlar, Germany). Excitation filters for fluorescein isothiocyanate (488 nm) and Texas-red (568 nm) were used. Three sections per mouse were selected and the distance between the two adjacent sections was 2 mm. Immunoreactivity was determined based on the integrated optical density of the immunostaining using Adobe Photoshop CS6 (Adobe Systems, San Jose, CA, USA).

Western blot assay

Western blot analysis was used to determine the levels of Aβ oligomers, tau protein, and five synaptic proteins (synapsin-1, dynamin 1, calpain, PSD-95,

and synaptophysin) in the right hemisphere from immunized mice. Protein samples were isolated on 12% sodium dodecyl sulfate polyacrylamide gel electrophoresis gel and transferred to a polyvinylidene fluoride membrane. In 20 mM Tris-HCl (pH 7.4) containing 150 mM NaCl and 0.05% Tween 20, the 10% skim milk-blocked membrane was washed with Tris-HCl (pH 7.4) containing 150 mM NaCl and 0.05% Tween 20. Then, antibody 6E10 (1:1500), tau5 (1:200, mouse anti-tau antibody, Cat# 10274-1-AP, RRID: AB80579, Thermo Fisher Scientific, Rockford, IL, USA), AT8 (Cat# 10274-1-AP, RRID: AB254409, mouse anti-paired helical filament (PHF) tau antibody, 1:200, Thermo Fisher Scientific), AT180 (Cat# 28866-1-AP, RRID: AB223192, mouse anti-PHF tau antibody, 1:500 Thermo Fisher Scientific), anti-dynamin 1 (Cat# C16, RRID: AB52661, 1:2000, mouse, Santa Cruz Biotechnology, Inc., Santa Cruz, CA, USA), anti-PSD-95 (Cat# 20665-1-AP, RRID: AB238135, 1:500, rabbit, Invitrogen, Carlsbad, CA, USA), anti-synaptophysin (Cat# L128, RRID: AB116659, rabbit, 1:500, Bioworld Technology, Inc., Bloomington, MN, USA), anti-synapsin-1 (Cat# 20508-1-AP, RRID: AB254349, 1:500, rabbit, Bioworld Technology, Inc.), anti-calpain (Cat# 10538-1-AP, RRID:AB170926 1:500, rabbit, MilliporeSigma), or anti-β-actin (Cat# 66009-1-Ig, mouse, 1:500, RRID: ab179467, MilliporeSigma) for 1 hour at 37°C. The membranes were then incubated with horseradish peroxidase-conjugated IgG (1:5000, goat, RRID: AB270144, Cat# SA00001-2, GBI, Bothell, WA, USA) for 0.5 hour at 37°C, and protein was detected with enhanced chemiluminescence reagents (ECL, Pierce, IL, USA). Density analysis was performed using the ImageJ software. The optical density was normalized to the PBS group.

Statistical analysis

No statistical methods were used to predetermine sample sizes; however, our sample sizes were similar to those reported in a previous publication (Zhang et al., 2021b). The evaluator was blinded to the animal group. One mouse died in the vaccine-immunized group and one died in the PBS-immunized group. All data are expressed as mean ± standard deviation (SD). The difference of immunological, neuropathological, and behavioral results between groups was analyzed using a one-way analysis of variance, followed by the Student-Newman-Keuls multiple range test using SPSS 19 (IBM Statistics, Armonk, NY, USA). A *P*-value < 0.05 was considered to indicate a statistically significant difference.

Results

Construction and confirmation of Aβ DNA vaccine

The p(Aβ3–10)10-MT vaccine was successfully constructed by Wanlei Life Sciences Corporation (Shenyang, China) as described by Sha et al. (2014). A graphic of the DNA construct and overall experimental diagram is shown in **Figure 1**.

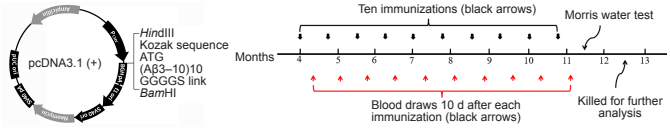

Figure 1 | **The structure of vaccine and design of the study.**
(A) Ten tandem repeats of complementary DNA for the human $A\beta_{3-10}$ gene were subcloned into the eukaryotic expression vector pcDNA3.1(+) using the restriction sites *Hin*dIII and *Eco*RI. (B) The whole flow chart of the study and a timeline of immunizations (black arrows), blood draws (red arrows), and when the mice were tested and sacrificed for additional further analysis.

The p(Aβ3–10)10-MT vaccine induces high anti-Aβ antibody levels against different AB conformations

The anti-Aβ antibody levels in the serum samples of mice were detected using ELISA. The anti-Aβ antibodies were detected in p(Aβ3–10)10-MT-immunized 3×Tg-AD mice, and no antibodies were observed in the PBS-injected mice. Peak antibody levels reached 47.05 ± 2.72 μg/mL in the p(Aβ3–10)10-MT group after the 10th vaccination and was sustained thereafter (**Figure 2A**). The antibody concentration was significantly higher in the p(Aβ3–10)10-MT group than in the PBS group ($P < 0.01$; **Figure 2B**). When mice were almost 13 months old, Aβ oligomers were extracted from the cerebral homogenates and analyzed using western blotting with the 6E10 antibody. The trimers, tetramers, hexamers, nonamers, dodecamers, and fibrils are represented by arrows in **Figure 2C**. The serum antibodies of p(Aβ3–10)10-MT-immunized mice strongly bound to $A\beta_{42}$ oligomers but minimally to $A\beta_{42}$ fibrils (**Figure 2C**). This result shows the p(Aβ3–10)10-MT serum antibodies recognize the Aβ oligomer depending on Aβ peptide conformation.

p(Aβ3–10)10-MT vaccine alleviates cognitive impairment in aged 3×Tg-AD mice

The Morris water maze test was used to evaluate cognition in the 3×Tg-AD and WT mice after the last vaccination. Compared with the PBS group, the escape latency for p(Aβ3–10)10-MT-immunized mice was significantly reduced at 3–5 days of training ($P < 0.01$; **Figure 3A**). In the probe test, compared with the PBS group, the p(Aβ3–10)10-MT group spent significantly more time in the target quadrant ($P < 0.01$; **Figure 3B**). The times crossing the target platform in the p(Aβ3–10)10-MT group was significantly increased compared with PBS group ($P < 0.01$; **Figure 3C**). The performance in the Morris water maze between mice in the p(Aβ3–10)10-MT and WT groups was not significantly different ($P > 0.05$). In summary, these data clearly indicate that early immunotherapy can effectively improve the cognitive function of aged 3×Tg-AD mice.

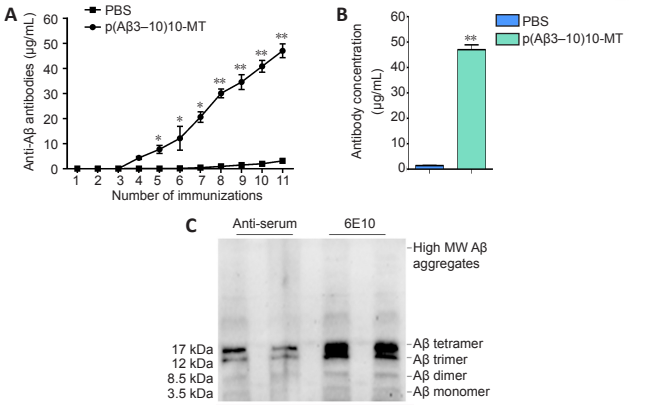

Figure 2 | **Levels and immunogenicity of the anti-Aβ antibody.**
(A) The anti-Aβ antibodies in the serum can be detected in p(Aβ3–10)10-MT immunized 3×Tg-AD mice ($n = 10$) while no antibody was discovered in the mice of the PBS group. Blood was drawn 11 times with the first occurring before the 10 immunizations which are labeled 2–11. (B) Antibody levels in the plasma were significantly higher in the p(Aβ3–10)10-MT-immunized group than those in the PBS group. Data are expressed as the mean ± SD ($n = 10$ mice in each group). *$P < 0.05$, **$P < 0.01$, *vs.* PBS group (one-way analysis of variance followed by Student-Newman-Keuls multiple range test). (C) The immunogenicity against different Aβ conformations. Aβ: Amyloid-beta; AD: Alzheimer's disease; MT: melatonin; MW: molecular weight; PBS: phosphate-buffered saline; Tg: transgenic.

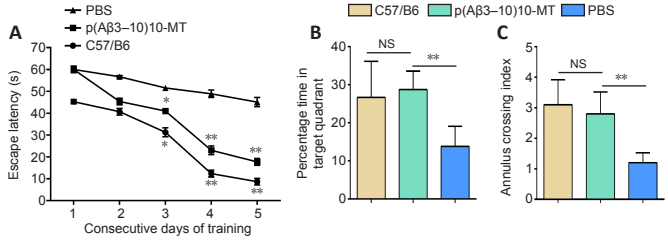

Figure 3 | **The new vaccine improves the cognitive function of 3×Tg-AD mice in the Morris water maze.**
(A) The escape latency in the hidden platform. In the hidden platform training days, the escape latency of the p(Aβ3–10)10-MT group was significantly shortened (except for the first day), compared with the PBS group. (B) Time in the target quadrant in the spatial probe trail. In the spatial probe trail, mice in the p(Aβ3–10)10-MT group spent more time in the target quadrant than mice in the PBS group. (C) Times crossing the original platform in the spatial probe trail. In the spatial probe trail, times crossing the original platform location were increased in the p(Aβ3–10)10-MT group, compared with the PBS group. Data are expressed as the mean ± SD ($n = 10$ mice in each group). *$P < 0.05$, **$P < 0.01$, *vs.* PBS group (one-way analysis of variance followed by Student-Newman-Keuls multiple range test). 3×Tg-AD mice: Amyloid precursor protein/presenilin-1/tau transgenic mouse models; Aβ: amyloid-beta; AD: Alzheimer's disease; MT: melatonin; PBS: phosphate-buffered saline; Tg: transgenic.

p(Aβ3–10)10-MT vaccine prevents plaque deposits through microglia activation

Immunohistochemistry was performed to evaluate the Aβ burden in the cortex and hippocampus of vaccinated and control mice. The Aβ amyloid plaque was significantly reduced to 41% in the cortex and 50 % in the hippocampus for the p(Aβ3–10)10-MT-immunized mice compared with PBS-injected mice (**Figure 4A**). Furthermore, ELISA results of cerebral homogenates showed that vaccine immunization markedly decreased the levels of soluble ($P < 0.05$) and insoluble ($P < 0.01$) $A\beta_{42}$ peptides in the cortex and hippocampus, respectively, compared with PBS-immunized mice (**Figure 4B**). Immunofluorescence results showed that the Aβ plaques were densely scattered and surrounded microglia with increased cytoplasm and longer synapses which tended to be activated in p(Aβ3–10)10-MT-immunized mice (**Figure 4C**), confirming the role of microglia in clearing the senile plaque deposition. Reductions in plaque load accompanied by reduced gliosis suggest that microglial activation is necessary for efficient removal of compact amyloid deposits with immunotherapy. Our fluorescence immunolabeling showed dark-brown, densely scattered Aβ plaque surrounded by activated microglial with increased cytoplasm and longer synapses which showed the activated tendency.

p(Aβ3–10)10-MT vaccine markedly reduces hyperphosphorylated forms of tau

Tau phosphorylation at Ser202 and Thr205 (the AT8 form of tau and at Th231 (the AT180 form of tau) promote pathological tau changes (Braak et al., 2006). Large numbers of hyperphosphorylated tau protein was observed in non-immunized 3×Tg-AD mice (McKee et al., 2008). After Aβ vaccination, AT8-positive neurons were reduced and the AT8 signal was not as strong in p(Aβ3–10)10-MT-immunized mice compared with the PBS-injected mice ($P < 0.01$; **Figure 5A** and **B**). The same pattern was observed for AT180 after immunization with p(Aβ3–10)10-MT (**Figure 5C** and **D**). Protein extracted from the right hemisphere was analyzed using western blotting to detect AT8, AT180, and total tau levels. Both relative protein expression levels of AT8 and AT180 were significantly reduced in vaccinated mice compared with the control mice ($P < 0.05$; **Figure 5E** and **F**).

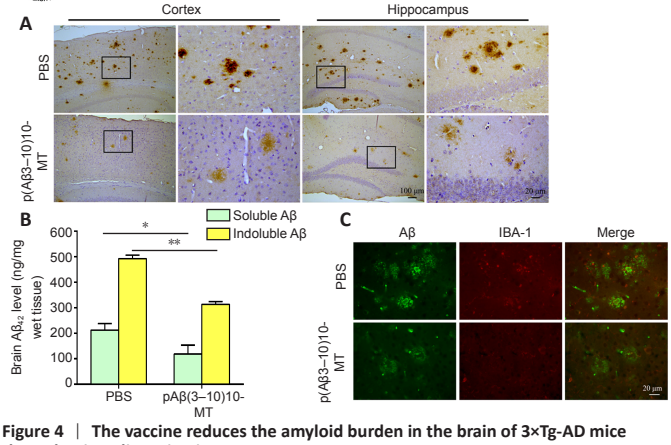

Figure 4 | The vaccine reduces the amyloid burden in the brain of 3×Tg-AD mice through microglia activation.

(A) Amyloid burden in both the cortex and hippocampus for the p(Aβ3–10)10-MT immunized mice was more greatly decreased than that in PBS-immunized mice by immunohistochemistry. (B) The levels of soluble and insoluble Aβ42 peptides were analyzed by enzyme-linked immunosorbent assay. Data are expressed as the mean ± SD (n = 10 mice in each group). *P < 0.05, **P < 0.01 (one-way analysis of variance followed by Student-Newman-Keuls multiple range test). (C) Fluorescein isothiocyanate showed Iba-1 positive cells (Texas-red: red) clustered around senile plaques (FITC: green) in the brain of p(Aβ3–10)10-MT immunized mice. Scale bars: 100 μm in original image in A, and 20 μm in enlarged part in A and B. 3×Tg-AD mice: Amyloid precursor protein/presenilin-1/tau transgenic mouse models; Aβ: amyloid-beta; AD: Alzheimer's disease; FITC: fluorescein isothiocyanate; MT: melatonin; PBS: phosphate-buffered saline; Tg: transgenic.

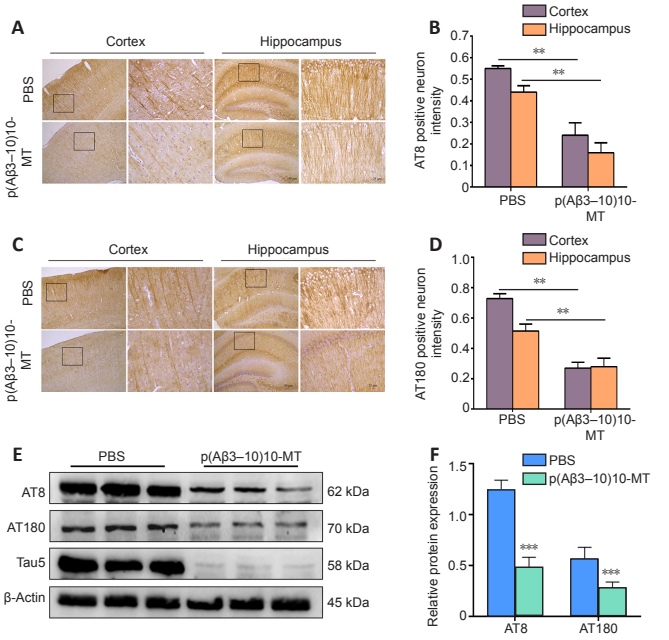

Figure 5 | The vaccine decreases the phosphorylated tau protein expression levels in the brains of 3×Tg-AD mice.

(A, B) AT8-positive neurons were more greatly reduced in both the cortex and hippocampus for the p(Aβ3–10)10-MT immunized mice than those in PBS-immunized mice by immunohistochemistry. (C, D) AT180-positive neurons were more greatly reduced in both the cortex and hippocampus for the p(Aβ3–10)10-MT immunized mice than those in PBS-immunized mice by immunohistochemistry. Data are expressed as the mean ± SD (n = 10 mice in each group). **P < 0.01 (one-way analysis of variance followed by Student-Newman-Keuls multiple range test). Scale bars: 100 μm in original image in A and C, and 20 μm in enlarged part in A and C. (E) Relative expression of AT8, and AT180, which was normalized to total tau by western blot. 3×Tg-AD mice: Amyloid precursor protein/presenilin-1/tau transgenic mouse models; Aβ: amyloid-beta; AD: Alzheimer's disease; ELISA: enzyme-linked immunosorbent assay; MT: melatonin; PBS: phosphate-buffered saline; Tg: transgenic.

p(Aβ3–10)10-MT vaccine prevents the loss of synaptic proteins and protects synaptic function

Reportedly, accumulation of Aβ can induce the activation of calpain, thereby degrading dynamin 1, a protein which promotes the release of synaptic vesicles (Fà et al., 2014) and post-synaptic density protein PSD-95, which is essential for synapse maturation and plasticity (Glasgow et al., 2020). Compared with C57/B6 mice of the same age, the expression levels of dynamin 1 and PSD-95 in the left hemisphere of untreated 3×Tg-AD mice were significantly reduced (P < 0.01) and those in the p(Aβ3–10)10-MT-immunized mice were not changed (P > 0.05). Similarly, the expression levels of synaptophysin and synapsin-1 were significantly reduced in the untreated group compared with those in the C57/B6 group (P < 0.01); however, p(Aβ3–10)10-MT immunization prevented protein decline compared with the PBS-injected group (P < 0.01; **Figure 6A**). Previous results showed that calpain was activated by Ca^{2+} influx induced by N-methyl-D-aspartate receptors, which promotes degradation of dynamin 1 and PSD-95 (Sinjoanu et al., 2008), leading to impaired memory function. **Figure 6B** showed that the p(Aβ3–10)10-MT could alleviate the decrease of synaptic related proteins. The calpain protein was decreased while the other four synaptic related proteins were protected from decreasing after the p(Aβ3–10)10-MT immunization.

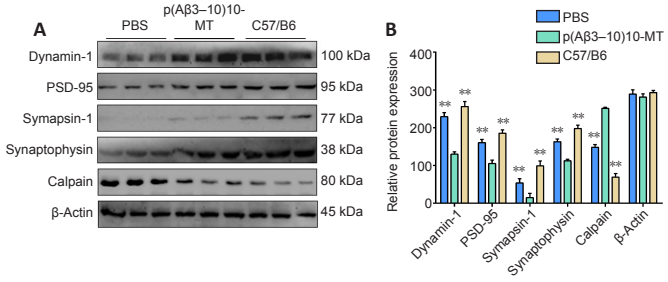

Figure 6 | The vaccine affects the synaptic protein expression in the left hemisphere of 3×Tg-AD mice.

(A) Western blot assay to identify the synaptic protein expression in the brain of mice. (B) Relative expression levels of the synaptic protein. Data are expressed as the mean ± SD (n = 10 mice in each group). *P < 0.05, **P < 0.01, $vs.$ p(Aβ3–10)10-MT vaccine group (one-way analysis of variance followed by Student-Newman-Keuls multiple range test). 3×Tg-AD mice: Amyloid precursor protein/presenilin-1/tau transgenic mouse models; Aβ: amyloid-beta; AD: Alzheimer's disease; MT: melatonin; PBS: phosphate-buffered saline; PSD95: postsynaptic density protein 95; Tg: transgenic.

p(Aβ3–10)10-MT vaccine prevents neuron loss in hippocampal CA3 area of 3×Tg-AD mice

Immunohistochemistry was used to detect the number of NeuN-positive neurons in the hippocampal CA3 area to evaluate the loss of neurons before and after immunization. The number of NeuN-positive neurons in hippocampal CA3 area of mice inoculated with the p(Aβ3–10)10-MT vaccine was significantly higher than that in the PBS group (P < 0.01; **Figure 7A** and **B**), indicating the vaccine had a protective effect against neuron loss in 3×Tg-AD mice.

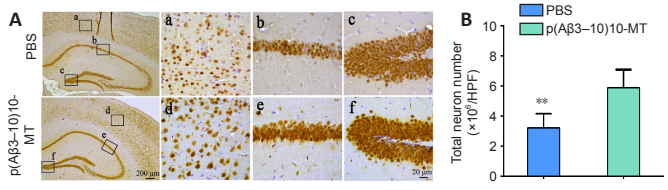

Figure 7 | The vaccine decreases the number of NeuN-positive neurons in right hemisphere of the brain in 3×Tg-AD mice.

(A) NeuN-positive neuron in mice of the two groups. (B) Total NeuN-positive neuron number in 20-fold field shows a 46 % loss in 3×Tg-AD mice immunized with PBS while only 11 % of neurons in mice immunized with p(Aβ3–10)10-MT was lost. Scale bars: 200 μm in the leftmost row, and 20 μm in the right three rows. Data are expressed as the mean ± SD (n = 10 mice in each group). **P < 0.01, $vs.$ p(Aβ3–10)10-MT vaccine group (one-way analysis of variance followed by Student-Newman-Keuls multiple range test). 3×Tg-AD mice: Amyloid precursor protein/presenilin-1/tau transgenic mouse models; Aβ: amyloid-beta; AD: Alzheimer's disease; MT: melatonin; PBS: phosphate-buffered saline; Tg: transgenic.

Microhemorrhages are rarely observed in the left hemisphere of p(Aβ3–10)10-MT vaccine-immunized mice

Prussian blue staining is used to label hemoglobin decomposition products containing hemosiderin (Searcy et al., 2021). As described in our previous study, microhemorrhages were detected in PBS- and p(Aβ3–10)10-MT-immunized Tg mice, ranging in size from large, diffuse areas, to small, single cell-sized blue profiles (Sha et al., 2014). Quantitative detection showed there was no obvious difference between the PBS-injected and p(Aβ3–10)10-MT-vaccinated groups (**Figure 8A** and **B**). Notably, microhemorrhages were rarely detected in the PBS-injected and p(Aβ3–10)10-MT-vaccinated mice.

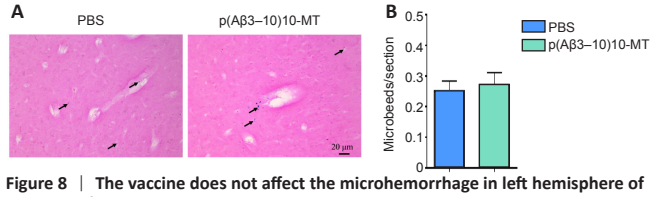

Figure 8 | The vaccine does not affect the microhemorrhage in left hemisphere of 3×Tg-AD mice.

(A) Prussian blue histological staining of the brain of PBS and p(Aβ3–10)10-MT immunized transgenic mice. Prussian blue histological staining represents that there was no obvious microhemorrhage in p(Aβ3–10)10-MT immunized transgenic mice. The arrows represent the hemosiderin deposits. Scale bars: 20 μm. (B) Microbleeds in 20-fold field. Data are expressed as the mean ± SD (n = 10 mice in each group), and were analyzed by one-way analysis of variance followed by Student-Newman-Keuls multiple range test. 3×Tg-AD mice: Amyloid precursor protein/presenilin-1/tau transgenic mouse models; Aβ: amyloid-beta; AD: Alzheimer's disease; MT: melatonin; PBS: phosphate-buffered saline; Tg: transgenicn.

Discussion

Active immunotherapies targeting Aβ have been widely performed in preclinical AD mouse model studies and human clinical trials (Lambracht-Washington and Rosenberg, 2012; Wisniewski and Goñi, 2015), however, significant clinical efficacy has not been achieved. The main reason may be the lack of specific methods to specifically target the most toxic components, Aβ oligomers (Lannfelt et al., 2014). Tau in the hippocampus of 3×Tg-AD mice reportedly decreased with the removal of Aβ plaques (Davtyan et al., 2019). Simply reducing soluble Aβ without changing soluble tau levels could not significantly improve cognitive ability, indicating that reversal of memory impairment requires the joint action of both factors (Schelle et al., 2019). Aβ has been proposed to activate Fyn phosphatase, a striatal-enriched protein tyrosine phosphatase, eventually inactivating Fyn and leading to the loss of synapses and dendritic spine collapse (Mairet-Coello et al., 2013). Together, these findings showed that Aβ may trigger AD pathogenesis and tau may be the decisive factor (Yu et al., 2012).

In previous studies, even high antibody titers in 18-month-old 3×Tg-AD mice after active immunotherapy could not completely reverse the deposition of Aβ and changes in cognitive function (Das et al., 2001; Acero et al., 2020). Notably, the sustained immune response may have further assisted in maintaining antibody-mediated clearance of Aβ and provided protection in 3×Tg-AD mice (Fulop et al., 2021). Another possibility for the decreased plaque clearance ability in elderly mice was the increased fibrillar composition and multiple factors, such as cross-linking, glycation, recombination, and integration, which promoted stronger plaques, all of which supported that early intervention therapy was more effective during incomplete plaque formation (Petrushina et al., 2017).

Compared with traditional peptide vaccines, DNA vaccines have many advantages such as being relatively safe, cost efficient, and able to maintain a reasonable level of antigen expression within cells. DNA vaccines can be easily manipulated to modify genes depending on the type of immune response required. However, because of the low efficiency of naked DNA transfection cells, the immunogenicity of DNA vaccines is low (Babiuk et al., 2003). The application of *in vivo* electroporation has been shown to increase the transfection efficacy and the immunogenicity of plasmid vaccines by several folds. With recent developments in electroporation systems for muscle delivery, the safety, tolerability, and clinically acceptable administration of DNA vaccines has advanced significantly (Allen et al., 2018). In the current study, induced anti-Aβ antibodies were immunoreactive to monomeric and oligomeric Aβ but reacted weakly with aggregated Aβ. p(Aβ3–10)10-MT immunotherapy through *in vivo* electroporation elicited high serum antibody titers that more strongly bound to oligomers than to monomers, effectively reducing Aβ peptide deposition and oligomers, which closely correlates with cognitive dysfunction and can eventually mitigate cognitive deficits. Our vaccine significantly increased the number of microglia clustered near amyloid plaques after immunotherapy, indicating that immune therapy could change the phagocytic function of microglia and promote plaque clearance. Our data show a significant reduction in tau phosphorylation after removal of amyloid. Immunization can reduce AT8 and AT180, thereby reducing tau-associated pathology which is the same as previous study (Pradeepkiran and Reddy, 2019).

Pre-synaptic and post-synaptic proteins are more strongly associated with cognitive deficits than Aβ plaques. The major determinant of synaptic plasticity is post-synaptic protein PSD-95. Dynamin 1 may be involved in synaptic vesicle release, which contributes to Aβ-induced synaptic pathology (Xia et al., 2017). After immunizing 3×Tg-AD mice with p(Aβ3–10)10-MT, the activation of calpain in the brain was significantly decreased, which may have led to the reduction of dynamin 1 and PSD-95 degradation, eventually protecting the synaptic function. In the present study, the loss of neurons in the vaccine group was significantly reduced and the health of neurons improved, indicating that immunization with our vaccine can partially protect against neuron loss in 3×Tg-AD mice. Because of the limited tissue of transgenic mice, we can consider to further explore the changes of tau oligomers in future studies.

In summary, the immunogenicity, efficacy, and mechanism of p(Aβ3–10)10-MT vaccine used as early immunotherapy in 3×Tg-AD mice were comprehensively described. Our data show that active immunization by *in vivo* electroporation with a DNA plasmid coding for $A\beta_{3-10}$ induces a humoral immune response against Aβ in 3×Tg-AD mice and significantly reduces tau as well as Aβ.

The novel vaccine presented in this study used Aβ oligomers as the specific target, reduced senile plaques and tau phosphorylation, and protected synapse function without microhemorrhages. Therefore, the vaccine can be considered an effective and safe candidate for preventive treatment or early immunotherapy in AD.

Acknowledgments: *We thank the experimental services and animal care from the Laboratory Animal Centre of China Medical University.*
Author contributions: *Study design: YPC, XLS; experimental implementation: SS, XNX, TW, YL; data analysis: LQ, RWZ; manuscript draft: SS, XNX, LQ. All the authors read and approved the final manuscript.*
Conflicts of interest: *The authors declare no conflicts of interest.*
Author statement: *This paper has been posted as a preprint on Research Square with doi:10.21203/rs.3.rs-92180/v1, which is available from: https://assets.researchsquare.com/files/rs-92180/v1/51811a0d-8669-4ca3-bad6-3a1ec50b352b.pdf?c=1603118158.*
Availability of data and materials: *All data generated or analyzed during this study are included in this published article and its supplementary information files.*

Open peer reviewer: *Nemil N. Bhatt, The University of Texas Medical Branch, USA.*
Additional file: *Open peer review report 1.*

References

Acero G, Garay C, Venegas D, Ortega E, Gevorkian G (2020) Novel monoclonal antibody 3B8 specifically recognizes pyroglutamate-modified amyloid β 3-42 peptide in brain of AD patients and 3×Tg-AD transgenic mice. Neurosci Lett 724:134876.

Allen A, Wang C, Caproni LJ, Sugiyarto G, Harden E, Douglas LR, Duriez PJ, Karbowniczek K, Extance J, Rothwell PJ, Orefo I, Tite JP, Stevenson FK, Ottensmeier CH, Savelyeva N (2018) Linear doggybone DNA vaccine induces similar immunological responses to conventional plasmid DNA independently of immune recognition by TLR9 in a pre-clinical model. Cancer Immunol Immunother 67:627-638.

Asuni AA, Boutajangout A, Scholtzova H, Knudsen E, Li YS, Quartermain D, Frangione B, Wisniewski T, Sigurdsson EM (2006) Vaccination of Alzheimer's model mice with Abeta derivative in alum adjuvant reduces Abeta burden without microhemorrhages. Eur J Neurosci 24:2530-2542.

Babiuk LA, Pontarollo R, Babiuk S, Loehr B, van Drunen Littel-van den Hurk S (2003) Induction of immune responses by DNA vaccines in large animals. Vaccine 21:649-658.

Braak H, Alafuzoff I, Arzberger T, Kretzschmar H, Del Tredici K (2006) Staging of Alzheimer disease-associated neurofibrillary pathology using paraffin sections and immunocytochemistry. Acta Neuropathol 112:389-404.

Dahlgren KN, Manelli AM, Stine WB, Jr., Baker LK, Krafft GA, LaDu MJ (2002) Oligomeric and fibrillar species of amyloid-beta peptides differentially affect neuronal viability. J Biol Chem 277:32046-32053.

Das P, Murphy MP, Younkin LH, Younkin SG, Golde TE (2001) Reduced effectiveness of Abeta1-42 immunization in APP transgenic mice with significant amyloid deposition. Neurobiol Aging 22:721-727.

Davtyan H, Hovakimyan A, Kiani Shabestari S, Antonyan T, Coburn MA, Zagorski K, Chailyan G, Petrushina I, Svystun O, Danhash E, Petrovsky N, Cribbs DH, Agadjanyan MG, Blurton-Jones M, Ghochikyan A (2019) Testing a MultiTEP-based combination vaccine to reduce Aβ and tau pathology in Tau22/5xFAD bigenic mice. Alzheimers Res Ther 11:107.

Fà M, Staniszewski A, Saeed F, Francis YI, Arancio O (2014) Dynamin 1 is required for memory formation. PLoS One 9:e91954.

Fukuchi K, Hart M, Li L (1998) Alzheimer's disease and heparan sulfate proteoglycan. Front Biosci 3:d327-337.

Fulop T, Tripathi S, Rodrigues S, Desroches M, Bunt T, Eiser A, Bernier F, Beauregard PB, Barron AE, Khalil A, Plotka A, Hirokawa K, Larbi A, Bocti C, Laurent B, Frost EH, Witkowski JM (2021) Targeting impaired antimicrobial immunity in the brain for the treatment of Alzheimer's disease. Neuropsychiatr Dis Treat 17:1311-1339.

Glasgow SD, Wong EW, Thompson-Steckel G, Marcal N, Séguéla P, Ruthazer ES, Kennedy TE (2020) Pre- and post-synaptic roles for DCC in memory consolidation in the adult mouse hippocampus. Mol Brain 13:56.

Godyń J, Jończyk J, Panek D, Malawska B (2016) Therapeutic strategies for Alzheimer's disease in clinical trials. Pharmacol Rep 68:127-138.

Holmes C, Boche D, Wilkinson D, Yadegarfar G, Hopkins V, Bayer A, Jones RW, Bullock R, Love S, Neal JW, Zotova E, Nicoll JA (2008) Long-term effects of Abeta42 immunisation in Alzheimer's disease: follow-up of a randomised, placebo-controlled phase I trial. Lancet 372:216-223.

Lambracht-Washington D, Rosenberg RN (2012) Active DNA Aβ42 vaccination as immunotherapy for Alzheimer disease. Transl Neurosci 3:307-313.

Lannfelt L, Relkin NR, Siemers ER (2014) Amyloid-ß-directed immunotherapy for Alzheimer's disease. J Intern Med 275:284-295.

Loureiro JC, Pais MV, Stella F, Radanovic M, Teixeira AL, Forlenza OV, de Souza LC (2020) Passive antiamyloid immunotherapy for Alzheimer's disease. Curr Opin Psychiatry 33:284-291.

Mairet-Coello G, Courchet J, Pieraut S, Courchet V, Maximov A, Polleux F (2013) The CAMKK2-AMPK kinase pathway mediates the synaptotoxic effects of Aβ oligomers through Tau phosphorylation. Neuron 78:94-108.

Martinez B, Peplow PV (2019) Amelioration of Alzheimer's disease pathology and cognitive deficits by immunomodulatory agents in animal models of Alzheimer's disease. Neural Regen Res 14:1158-1176.

McKee AC, Carreras I, Hossain L, Ryu H, Klein WL, Oddo S, LaFerla FM, Jenkins BG, Kowall NW, Dedeoglu A (2008) Ibuprofen reduces Abeta, hyperphosphorylated tau and memory deficits in Alzheimer mice. Brain Res 1207:225-236.

Nisbet RM, Polanco JC, Ittner LM, Götz J (2015) Tau aggregation and its interplay with amyloid-β. Acta Neuropathol 129:207-220.

Oddo S, Vasilevko V, Caccamo A, Kitazawa M, Cribbs DH, LaFerla FM (2006) Reduction of soluble Abeta and tau, but not soluble Abeta alone, ameliorates cognitive decline in transgenic mice with plaques and tangles. J Biol Chem 281:39413-39423.

Palmeri A, Ricciarelli R, Gulisano W, Rivera D, Rebosio C, Calcagno E, Tropea MR, Conti S, Das U, Roy S, Pronzato MA, Arancio O, Fedele E, Puzzo D (2017) Amyloid-β peptide is needed for cGMP-induced long-term potentiation and memory. J Neurosci 37:6926-6937.

Panza F, Lozupone M, Seripa D, Imbimbo BP (2019) Amyloid-β immunotherapy for alzheimer disease: is it now a long shot? Ann Neurol 85:303-315.

Percie du Sert N, Hurst V, Ahluwalia A, Alam S, Avey MT, Baker M, Browne WJ, Clark A, Cuthill IC, Dirnagl U, Emerson M, Garner P, Holgate ST, Howells DW, Karp NA, Lazic SE, Lidster K, MacCallum CJ, Macleod M, Pearl EJ, et al. (2020) The ARRIVE guidelines 2.0: Updated guidelines for reporting animal research. PLoS Biol 18:e3000410.

Petrushina I, Davtyan H, Hovakimyan A, Davtyan A, Passos GF, Cribbs DH, Ghochikyan A, Agadjanyan MG (2017) Comparison of efficacy of preventive and therapeutic vaccines targeting the N terminus of β-amyloid in an animal model of Alzheimer's disease. Mol Ther 25:153-164.

Pradeepkiran JA, Reddy PH (2019) Structure based design and molecular docking studies for phosphorylated tau inhibitors in Alzheimer's disease. Cells 8:260.

Rajamohamedsait HB, Sigurdsson EM (2012) Histological staining of amyloid and pre-amyloid peptides and proteins in mouse tissue. Methods Mol Biol 849:411-424.

Schelle J, Wegenast-Braun BM, Fritschi SK, Kaeser SA, Jährling N, Eicke D, Skodras A, Beschorner N, Obermueller U, Häsler LM, Wolfer DP, Mueggler T, Shimshek DR, Neumann U, Dodt HU, Staufenbiel M, Jucker M (2019) Early Aβ reduction prevents progression of cerebral amyloid angiopathy. Ann Neurol 86:561-571.

Schneider CA, Rasband WS, Eliceiri KW (2012) NIH Image to ImageJ: 25 years of image analysis. Nat Methods 9:671-675.

Schommer NN, Nguyen J, Yung BS, Schultheis K, Muthumani K, Weiner DB, Humeau L, Broderick KE, Smith TRF (2019) Active immunoprophylaxis and vaccine augmentations mediated by a novel plasmid DNA formulation. Hum Gene Ther 30:523-533.

Searcy K, Rainwater S, Jeroudi M, Baliga R (2021) Erythropoietin-stimulating agent-resistant vitamin B(6) deficiency anemia in a pediatric patient on hemodialysis. Pediatr Nephrol 36:473-476.

Sevigny J, Chiao P, Bussière T, Weinreb PH, Williams L, Maier M, Dunstan R, Salloway S, Chen T, Ling Y, O'Gorman J, Qian F, Arastu M, Li M, Chollate S, Brennan MS, Quintero-Monzon O, Scannevin RH, Arnold HM, Engber T, et al. (2016) The antibody aducanumab reduces Aβ plaques in Alzheimer's disease. Nature 537:50-56.

Sha S, Xing XN, Cao YP (2014) Active immunotherapy facilitates Aβ plaque removal following through microglial activation without obvious T cells infiltrating the CNS. J Neuroimmunol 274:62-70.

Sinjoanu RC, Kleinschmidt S, Bitner RS, Brioni JD, Moeller A, Ferreira A (2008) The novel calpain inhibitor A-705253 potently inhibits oligomeric beta-amyloid-induced dynamin 1 and tau cleavage in hippocampal neurons. Neurochem Int 53:79-88.

Wang CY, Wang T, Zheng W, Zhao BL, Danscher G, Chen YH, Wang ZY (2010) Zinc overload enhances APP cleavage and Aβ deposition in the Alzheimer mouse brain. PLoS One 5:e15349.

Wang JC, Zhu K, Zhang HY, Wang GQ, Liu HY, Cao YP (2020) Early active immunization with Aβ(3-10)-KLH vaccine reduces tau phosphorylation in the hippocampus and protects cognition of mice. Neural Regen Res 15:519-527.

Wisniewski T, Goñi F (2015) Immunotherapeutic approaches for Alzheimer's disease. Neuron 85:1162-1176.

Xia Z, Wang F, Zhou S, Zhang R, Wang F, Huang JH, Wu E, Zhang Y, Hu Y (2017) Catalpol protects synaptic proteins from beta-amyloid induced neuron injury and improves cognitive functions in aged rats. Oncotarget 8:69303-69315.

Yepes M (2021) The plasminogen activating system in the pathogenesis of Alzheimer's disease. Neural Regen Res 16:1973-1977.

Yu W, Polepalli J, Wagh D, Rajadas J, Malenka R, Lu B (2012) A critical role for the PAR-1/MARK-tau axis in mediating the toxic effects of Aβ on synapses and dendritic spines. Hum Mol Genet 21:1384-1390.

Yu YZ, Li QL, Wang HC, Liu S, Pang XB, Xu Q, Zhou XW, Huang PT (2018) Improved synaptic and cognitive function in aged 3 × Tg-AD mice with reduced amyloid-β after immunotherapy with a novel recombinant 6Aβ15-TF chimeric vaccine. Clin Immunol 193:12-23.

Zhang HY, Zhu K, Meng Y, Ding L, Wang JC, Yin WC, Yan Y, Cao YP (2018) Reduction of amyloid beta by Aβ3-10-KLH vaccine also decreases tau pathology in 3×Tg-AD mice. Brain Res Bull 142:233-240.

Zhang XM, Ouyang YJ, Yu BQ, Li W, Yu MY, Li JY, Jiao ZM, Yang D, Li N, Shi Y, Xu YY, He ZJ, Wang D, Yue H, Fu J (2021a) Therapeutic potential of dental pulp stem cell transplantation in a rat model of Alzheimer's disease. Neural Regen Res 16:893-898.

Zhang XY, Meng Y, Yan XJ, Liu S, Wang GQ, Cao YP (2021b) Immunization with Aβ3-10-KLH vaccine improves cognitive function and ameliorates mitochondrial dysfunction and reduces Alzheimer's disease-like pathology in Tg-APPswe/PSEN1dE9 mice. Brain Res Bull 174:31-40.

P-Reviewer: Bhatt NN; C-Editor: Zhao M; S-Editors: Yu J, Li CH; L-Editors: Yu J, Song LP; T-Editor: Jia Y